JOURNAL OF MODERN SCIENCE
SPECIAL ISSUE
3/57/2024
www.jomswsge.com

DOI: doi.org/10.13166/jms/191304

PRZEMYSŁAW ADAMKIEWICZ
WSEI University in Lublin, Poland
ORCID iD: orcid.org/0000-0003-3425-9566

MAŁGORZATA LALAK-DYBAŁA
WSEI University in Lublin, Poland
ORCID iD: orcid.org/0000-0001-5694-3460

ARKADIUSZ MAŁEK
WSEI University in Lublin, Poland
ORCID iD: orcid.org/0000-0001-7772-2755

THE USE OF NON-INVASIVE TOMOGRAPHIC IMAGING TO MONITOR LUNG CONDITION

ZASTOSOWANIE NIEINWAZYJNEGO OBRAZOWANIA TOMOGRAFICZNEGO DO MONITOROWANIA STANU PŁUC

Abstract

The development of ultrasound tomography (UST) aimed to significantly enhance the precision and safety of non-invasive UST imaging, particularly for studying crystallization processes in biological tissues. The initiative sought to address the limitations of previous versions by incorporating advanced technological upgrades and providing a more user-friendly interface. The revised system comprises eight four-channel measurement cards interconnected via a high-speed FD CAN bus capable of 8 MBPS data transfer. Each card features a dedicated square wave generator, band-pass filters tailored to specific ultrasonic transducer frequencies, and a sophisticated signal envelope processing unit. The core processing unit is built around a 32-bit STM32G474RE microcontroller, ensuring robust data handling and image reconstruction capabilities. The UST device presented demonstrates improved image clarity and reduced noise interference. The measurement card redesign has achieved a sampling rate of 4 MBPS per channel and includes a two-stage amplification for dynamic range management. Upgraded power components, comprehensive shielding, and the integration of advanced analog switches have led to an enhanced signal-to-noise ratio, pivotal for high-resolution imaging. The advancements presented in the UST device mark a noteworthy progression in ultrasound imaging technology, extending beyond traditional applications. High-speed data collection, precise signal processing, and user-centered design have all come together to make a system that can image crystallization processes more accurately and accurately over and over again. The integration of a robust control unit with a Raspberry Pi-based interface has streamlined the imaging process, making it more accessible and adaptable to a variety of research and clinical scenarios. This project sets a new standard for ultrasound imaging systems and opens avenues for further innovations in the field.

Streszczenie

Opracowanie ulepszonego tomografu ultradźwiękowego (UST) miało na celu znaczne zwiększenie precyzji i bezpieczeństwa nieinwazyjnego obrazowania UST, szczególnie w przypadku badania procesów krystalizacji w tkankach biologicznych. Inicjatywa ta miała na celu wyeliminowanie ograniczeń poprzednich wersji poprzez wprowadzenie zaawansowanych ulepszeń technologicznych i zapewnienie bardziej przyjaznego dla użytkownika interfejsu. Zmieniony system składa się z ośmiu czterokanałowych kart pomiarowych, połączonych ze sobą za pomocą szybkiej magistrali FD CAN zdolnej do przesyłania danych z prędkością 8 MBPS. Każda karta posiada dedykowany generator fali prostokątnej, filtry pasmowo-przepustowe dostosowane do określonych częstotliwości przetworników ultradźwiękowych oraz zaawansowaną jednostkę przetwarzania obwiedni sygnału. Podstawowa jednostka przetwarzająca jest

zbudowana na bazie 32-bitowego mikrokontrolera STM32G474RE, zapewniając obsługę danych i możliwości rekonstrukcji obrazu. Prezentowany tomograf UST charakteryzuje się lepszą klarownością obrazu i zmniejszonymi zakłóceniami. Przeprojektowana karta pomiarowa osiągnęła częstotliwość próbkowania 4 MBPS na kanał i zawiera dwustopniowe wzmocnienie do zarządzania zakresem dynamicznym. Ulepszone komponenty zasilania, kompleksowe ekranowanie i integracja zaawansowanych przełączników analogowych doprowadziły do poprawy stosunku sygnału do szumu, co ma kluczowe znaczenie dla obrazowania w wysokiej rozdzielczości. Rozwiązania zaprezentowane w tomografie UST są dowodem postępu w technologii obrazowania ultrasonograficznego, wykraczający poza tradycyjne zastosowania. Takie cechy jak szybkie gromadzenie danych, precyzyjne przetwarzanie sygnału i konstrukcja zorientowana na użytkownika zostały połączone w celu stworzenia spójnego systemu, który może dokładniej obrazować procesy krystalizacji. Integracja jednostki sterującej z interfejsem opartym na Raspberry Pi usprawniła proces obrazowania, czyniąc go bardziej dostępnym i łatwiejszym do dostosowania do różnych scenariuszy badawczych i klinicznych. Opisany projekt wyznacza nowy standard dla systemów obrazowania ultrasonograficznego i otwiera drogę do dalszych innowacji w tej dziedzinie.

Keywords: *Ultrasound Tomography, Non-invasive Imaging, Crystallization Processes, Signal Processing, Medical Diagnostics*

Słowa kluczowe: *tomografia ultradźwiękowa, obrazowanie nieinwazyjne, procesy krystalizacji, przetwarzanie sygnałów, diagnostyka medyczna*

Introduction

Lung conditions encompass a broad spectrum of disorders affecting millions worldwide, posing significant healthcare burdens (Yetisen et al., 2018). These conditions can be classified into obstructive types, such as asthma and chronic obstructive pulmonary disease (COPD), which restrict airflow, and restrictive types, such as fibrosis, which impair the expansion of the lungs (Rymarczyk, 2019). Additionally, infectious diseases such as tuberculosis and pneumonia continue to pose serious health threats, particularly in low-resource settings (Soleimani Rymarczyk, 2023). The complexity and variability of lung diseases necessitate precise and dynamic monitoring strategies to optimize treatment outcomes. While effective for diagnostic assessments, traditional monitoring techniques often need to improve in providing real-time,

continuous data essential for managing acute episodes and adjusting treatments. For example, spirometry, the standard tool for assessing lung function, requires active participation from patients, which can be challenging during severe respiratory distress (Mazurek et al., 2020). Moreover, the inherent limitations of radiographic methods such as X-rays and CT scans, including radiation exposure, cost, and the need for specialized facilities, restrict their frequent use (Nagafune et al., 2014). This is particularly problematic in chronic conditions where ongoing monitoring is pivotal. There is also an increasing awareness of the risks associated with repeated radiation exposure, particularly in children and young adults who are more susceptible to radiation-induced complications. The advent of innovative monitoring techniques that are non-invasive, safe, and capable of delivering instant feedback on the patient's lung health could transform the management of pulmonary diseases (Laitinen et al., 2008; Zhao et al., 2019). In this regard, ultrasound tomography stands out as an up-and-coming technology. It eliminates the risks associated with radiation, offers portability, and provides a detailed view of the lung's morphology and function under various physiological and pathological conditions. This capability to monitor changes over time, even at the bedside, makes it an invaluable tool in acute and chronic care settings, leading to more personalized and responsive treatment strategies.

Ultrasound tomography represents a significant advancement in medical imaging, particularly for lung monitoring (Mazurek et al., 2020; Zhang et al., 2016). This technology utilizes sound waves at medical ultrasound frequencies to produce detailed images of internal body structures, including soft tissues that are typically challenging to image with conventional ultrasound. In lung imaging, ultrasound tomography is especially promising because it provides high-resolution images that reveal subtle changes in lung tissue and fluid accumulation without ionizing radiation. (Dai et al., 2023; Tutschek et al., 2017). The principle behind ultrasound tomography is the transmission and reception of ultrasound waves from multiple angles through the patient's body. Unlike conventional ultrasound, which primarily images the reflection of sound waves from structures, ultrasound tomography measures both the reflection and transmission of sound waves (Bal et al., 2015; Cueto et al., 2021; Khairi et al., 2019). This dual approach creates a three-dimensional image of the lung's

internal structure. It captures tissue density and composition variations with greater clarity and detail than standard ultrasound techniques. One of the critical advantages of ultrasound tomography for lung monitoring is its safety and non-invasiveness. It can be used repeatedly for patients who require ongoing monitoring, such as those with chronic lung diseases or post-operative patients. The portability of ultrasound devices also adds a layer of convenience, enabling in-situ imaging in intensive care units, emergency rooms, or even in remote or rural settings where large radiographic equipment is impractical. Furthermore, ultrasound tomography can be integrated into telehealth frameworks, allowing for remote diagnostics and monitoring (Javaherian et al., 2020; Koulountzios et al., 2021). This integration is particularly advantageous during the COVID-19 pandemic, where minimizing patient movement and hospital visits is crucial. Real-time imaging capabilities facilitate immediate clinical decision-making, enhancing patient care by allowing for timely interventions. Overall, introducing ultrasound tomography into lung health monitoring could lead to a paradigm shift in how respiratory conditions are managed and treated, emphasizing preventive and continuous care approaches tailored to individual patient needs. This technology bridges the gap between diagnostic precision and safety and aligns with the evolving demands of modern healthcare systems for accessibility and patient-centric interventions.

Principles of Ultrasound Tomography

Ultrasound tomography technology utilizes sophisticated hardware and diverse operational modes to produce detailed images of internal body structures. The hardware setup for ultrasound tomography typically includes a series of transducers arranged in a circular or semi-circular array around the area of interest, such as the chest area for lung imaging. These transducers emit and receive ultrasound waves, capturing comprehensive cross-sectional data from multiple angles.

In medical imaging, ultrasound tomography emerges as a potent tool, particularly for applications that necessitate frequent and meticulous monitoring of lung conditions, all while shielding patients from harmful radiation. This powerful capability is created by harmoniously integrating advanced hardware

components and versatile operation modes. The transducer array is at the heart of the hardware, a critical element that houses numerous ultrasound transducers. Each transducer can be independently controlled, and their density and arrangement are paramount in achieving high-resolution images. The data acquisition system works in tandem with the transducer array. This system is tasked with processing the ultrasound signals received by the transducers. Designed to handle the vast amount of data generated during each scan, it ensures accurate image reconstruction, thereby playing a crucial role in the imaging process. Complementing these components is imaging software with advanced algorithms that interpret ultrasound data to construct detailed images. This software can uniquely differentiate between various types of tissue based on their acoustic properties, enhancing the images' clarity and usefulness.

Three distinct modes characterize the operation of ultrasound tomography. Like traditional ultrasound, the Reflection Mode interprets the echoes of ultrasound waves reflected from tissues. While it helps assess superficial structures, it can also contribute to deeper tissue imaging when combined with other modes. On the other hand, the Transmission Mode allows ultrasound waves to pass through the body from one transducer to another, capturing the transmission properties of the tissues they encounter. This method proves particularly valuable for imaging complex structures like the lungs, as it provides information about tissue density and composition. The third mode, compound imaging, combines reflection and transmission data to offer a more comprehensive view. Mitigating the limitations of each mode enhances contrast and resolution, providing a more detailed and accurate depiction of lung tissues.

Ultrasound tomography also supports real-time imaging, allowing clinicians to observe dynamic changes within the lungs as the patient breathes. This capability is critical for real-time assessment of lung function and treatment effectiveness. Furthermore, functional imaging can use the technology to assess lung tissue structure and physiological behavior, such as blood flow and fluid dynamics. This further extends its utility in clinical diagnostics and treatment monitoring. Combining these advanced hardware components and versatile operation modes endows ultrasound tomography with immense power and potential in medical imaging. It stands as a testament to the advancements

in medical technology, promising a future where diagnosis and treatment monitoring are more accurate, efficient, and safe.

As an advanced imaging modality, ultrasound tomography offers several advantages over traditional imaging techniques such as X-rays and computed tomography (CT) scans, especially when monitoring pulmonary conditions. The essence of its superiority lies not only in its safety and non-invasive nature but also in its adaptability and operational efficiency. One of the foremost benefits of ultrasound tomography is the absence of ionizing radiation, which is a significant concern with both X-rays and CT scans (Romanowski et al., 2019; Shanghai et al., 2021). The safety profile of ultrasound makes it an ideal choice for vulnerable populations, including pregnant women, children, and patients requiring frequent monitoring. This radiation-free approach allows for repeated use without the associated risks of cumulative radiation exposure, a factor particularly pertinent in chronic lung disease management, where continuous assessment is often necessary. Moreover, ultrasound equipment is inherently more portable and less costly than traditional radiographic machinery. This portability enables the use of ultrasound in hospital settings, outpatient clinics, and remote locations where large, stationary equipment is unavailable. In critical care environments, the ability to perform bedside imaging is invaluable, reducing the need to move critically ill patients and thus minimizing risks and discomfort. Ultrasound tomography also excels in its capacity for real-time imaging (Soleimani Rymarczyk, 2023; Tan et al., 2023; Wilson Patwari, 2010; Yigitler et al., 2017). As they operate, clinicians can observe the functional aspects of the lungs, watching the interplay of tissues with each breath. This immediate feedback is crucial for making rapid clinical decisions, particularly in emergency and acute care settings (Qiu et al., 2021; Schork, 2018). It also enhances the clinician's ability to monitor treatment efficacy over time, adjusting therapies in response to real-time observations of lung function. In addition to its diagnostic capabilities, ultrasound facilitates a deeper understanding of lung tissue physiological and pathological changes by allowing for functional assessments not readily available through X-rays or CT scans. For example, ultrasound can assess blood flow and fluid dynamics within the lungs, providing insights critical for managing conditions like pulmonary edema or heart failure. Ultrasound tomography is very useful

because it combines detailed imaging with functional assessment. It fills the gap between traditional methods that only give static pictures of the body and the living systems' constantly changing processes. This holistic approach enhances diagnostic accuracy and informs a more nuanced treatment strategy tailored to the individual's real-time medical needs. Overall, the comparative advantages of ultrasound tomography underscore its potential to revolutionize the field of pulmonary diagnostics and monitoring. By delivering safer, more accessible, and dynamically informative imaging solutions, ultrasound tomography is poised to become an indispensable tool in modern medical practice, particularly for conditions where the lungs are involved. This technology embodies the cutting edge of patient-centered care, where safety, efficiency, and precision are paramount.

Methodologies for Lung Monitoring

Ultrasound tomography (UST) procedures for imaging the lungs represent a fusion of advanced technology and meticulous technique tailored to address the challenges of visualizing such a complex and dynamic organ. Unlike traditional ultrasound, which is hindered by the lung's air content, UST leverages sophisticated methods to create detailed images of lung tissues. The process begins with patient preparation, where they are positioned to optimize access to the thoracic area, accommodating various postures such as sitting, standing, or lying down based on the patient's comfort and clinical needs. This flexibility is crucial, particularly for imaging patients who are critically ill and may not tolerate the conventional positioning required by other imaging modalities. Following patient positioning, a skilled technician applies a specialized conductive gel over the chest area. This gel is essential because it serves as a medium that promotes ultrasound wave transmission, eliminating potential air pockets between the transducers and the skin, which can distort the sound waves. The core of the UST system is its array of transducers strategically placed around the patient's thorax. These transducers can emit and receive ultrasound waves at frequencies optimized for deep-tissue penetration and fine-resolution imaging. Once activated, the system emits ultrasound waves

that travel through the thoracic structures, encountering tissues such as the pleura, lung parenchyma, and chest wall. UST is distinctive in its ability to capture both the reflection and transmission of these sound waves, providing a dual layer of data that enhances the image quality. The reflected waves give insight into the surface structures and boundaries, while the transmitted waves offer deeper insights into the tissue density and composition. This data is instantaneously relayed to a sophisticated computer system with advanced algorithms to reconstruct the waves into precise, high-resolution images. These images can reveal various lung conditions, from fluid accumulations and infections to structural anomalies like cysts or tumors. Throughout the scanning process, adjustments to the transducer's frequency and intensity settings are routinely made to adapt to the specific imaging needs, enhancing the depth and clarity of the images produced. In cases where lung function needs to be assessed, dynamic scanning techniques are employed. This involves capturing real-time images or video sequences of the lung tissues as they move during respiration, providing valuable information on lung mechanics and function critical for diagnosing and managing conditions like pulmonary fibrosis or chronic obstructive pulmonary disease. UST procedures are non-invasive, require minimal preparation, and are generally painless for the patient, encompassing only a few minutes of actual scanning time. The absence of radiation exposure is a significant advantage, particularly for populations requiring frequent monitoring, such as those with chronic lung diseases or children. Ultrasound tomography combines advanced imaging technology with precise procedures to provide a complete and safe way to image the lungs. This makes diagnosing problems easier and better managing patients by giving doctors timely, accurate, and detailed information. His method marks a significant advancement in pulmonary diagnostics, reflecting the evolution of medical imaging toward more patient-friendly and informative technologies.

Case Studies and Results

Figure 1 depicts a chest phantom setup for evaluating ultrasound tomography (UST) technology. This phantom, designed to simulate human thoracic anatomy, serves as a test subject for refining and demonstrating the capabilities of UST procedures. In panel (a), the top view of the phantom, we observe the circular arrangement of the transducer array, which is central to the UST system. The transducers are placed equidistantly along the phantom's curvature, mimicking the positioning around a human torso.

Figure 1. *View of the chest phantom with electrodes in place: (a) – top view, (b) – side view*

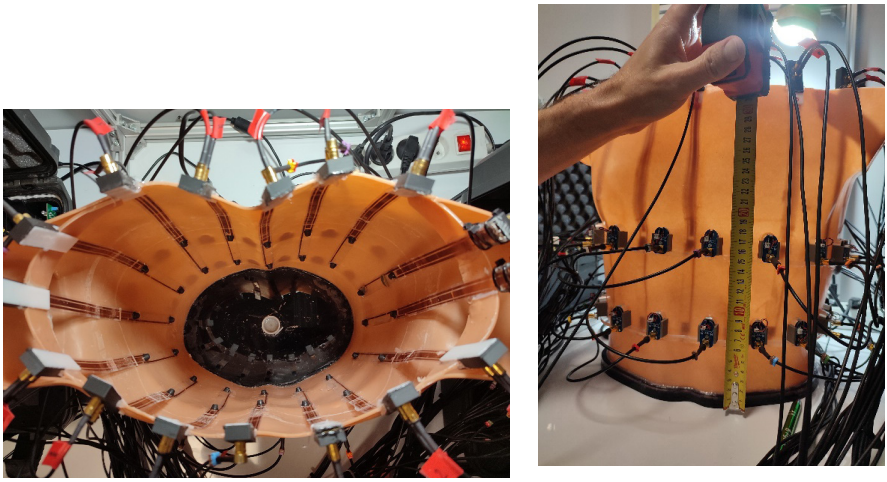

(a) **(b)**

This array is crucial for the multilateral transmission and reception of ultrasound waves, enabling the capture of comprehensive cross-sectional data. The labeled markers on the transducers are likely used for calibration and orientation purposes, ensuring precise data collection and imaging. Panel (b) offers a side view of the phantom, showcasing a more practical setup aspect. The tape measure held against the phantom is a tool for validating the dimensions and ensuring that the scale of the phantom matches typical human anatomy. This attention to detail is essential for the accuracy of the

UST procedure, as it guarantees that the data acquired from the phantom can be reliably extrapolated to clinical scenarios. The intricate network of cables stemming from the transducers demonstrates the complexity of data acquisition in UST. Each transducer is connected to the data processing unit, signifying the high level of detail captured during the imaging process. The precise nature of this setup underscores the potential of UST to revolutionize lung imaging by providing detailed insights into lung structure and function that surpass traditional imaging modalities.

The setup of ultrasonic transducers and graphite electrodes on two separate measuring rings for ultrasound tomography (UST) and electrical impedance tomography (EIT) studies is shown in Figure 2. The schematic denotes the lower measuring ring in panel (a) and the upper measuring ring in panel (b), providing a clear blueprint of the setup for these diagnostic modalities. In both panels, the blue dots represent EIT electrodes, which measure electrical conductivity throughout the thorax, capturing the distribution of various tissue types based on their electrical impedance. The red dots symbolize UST transducers, which emit and receive ultrasound waves, facilitating the creation of detailed images based on sound wave propagation and reflection within the chest cavity. The numbering next to each dot indicates the specific placement of electrodes and transducers, which are critical for data acquisition and subsequent reconstruction into images or impedance maps. Notably, the numbering direction for EIT differs from that of the UST, suggesting that the data collection for each modality may proceed in contrasting guidance. This directional distinction could be fundamental to how each modality constructs its respective imaging outputs, accounting for each technology's physical principles. The graphical representation in Figure 2 guides the precise placement and organization of the components necessary for UST and EIT procedures. Such an arrangement is critical to ensuring comprehensive coverage and high-resolution imaging of the thoracic region, allowing for accurate diagnostic assessments of lung conditions using these advanced non-invasive imaging technologies.

Figure 2. *Arrangement of ultrasonic transducers and graphite electrodes: (a) – lower measuring ring, (b) – upper measuring ring*

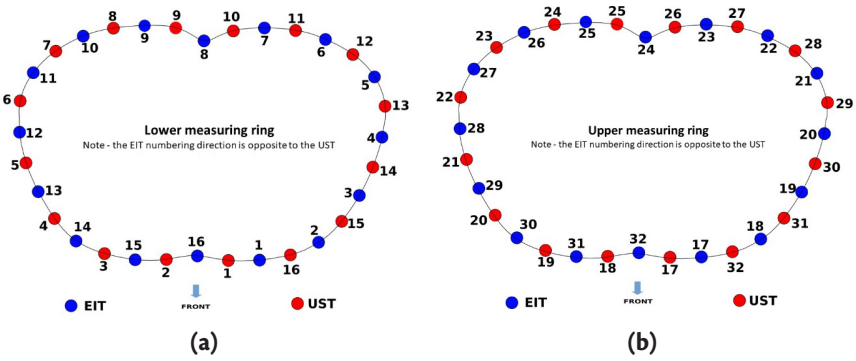

Figure 3 depicts the chest phantom used in calibrating and testing ultrasound tomography (UST) and electrical impedance tomography (EIT) technologies, illustrating the practical application of the setup shown in Figure 2. This phantom mimics the human chest, allowing a controlled environment to test UST and EIT systems' imaging capabilities and accuracy. The phantom has a vertical orientation, and measurements are provided to indicate scale. The blue dots represent the EIT electrodes, strategically placed at specific heights—170 millimeters at the top and 80 millimeters at the bottom. These electrodes are essential for EIT because they measure the electrical impedance across the chest phantom. This impedance is affected by the different conductive properties of the simulated tissues inside the phantom. Red dots indicate the placement of UST transducers. These are also placed at particular vertical intervals, marked by measurement lines labeled with arrows and numbers, such as 50, 52, 54, and so on, indicating the distance in millimeters between each transducer. The UST transducers are essential for sending and receiving ultrasound waves that penetrate the phantom, allowing the UST system to construct a detailed visual representation of what lies within. The arrangement of the transducers and electrodes, as shown in the figure, is critical to the functionality of the UST and EIT systems. Precise positioning ensures that the systems can collect comprehensive data, which is later processed to generate accurate images or impedance maps of the thoracic region.

This detailed setup is a testament to the intricate and thoughtful engineering behind modern diagnostic imaging technologies, reflecting their ability to replicate complex physiological structures to advance medical imaging and diagnostics.

Figure 3. *Chest phantom with ultrasound transducers and electrodes in place*

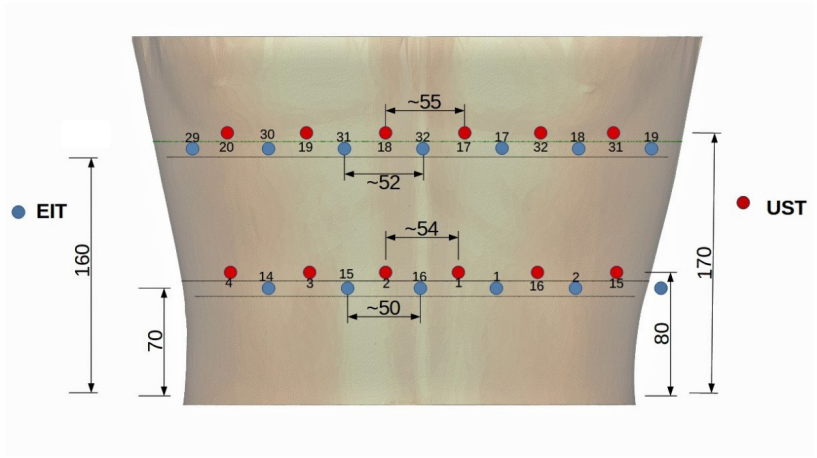

Figure 4 showcases the UST (Ultrasound Tomography) device in a panel view, providing a glimpse into the technological interface that powers the UST system. Enclosed within a robust case, which ensures both portability and protection for the delicate equipment inside, the device appears ready for field deployment or use in various clinical settings. The central processing unit is at the heart of the device, which features a display screen that serves as a user interface for operating the system. This screen may display real-time data, system diagnostics, and user controls, allowing for on-the-fly adjustments and monitoring during the UST procedure. Below the screen, an array of connectors is visible, corresponding to the ports into which the transducer cables are plugged. These connectors are likely numbered or coded in some fashion, corresponding to the individual transducers wrapped around the chest phantom. This ensures that each transducer's data can be accurately tracked and processed. The organized layout of the connectors suggests a systematic approach to data acquisition, which is crucial for reconstructing the complex three-dimensional images that UST is known for. The panel also includes LED

indicators next to each connector, which may serve as a status indicator to confirm active connections or flag any issues with specific transducers during the imaging process. As seen from the panel view in Figure 4, this UST device integrates advanced ultrasound imaging technology into a compact and user-friendly format. It is the conduit through which the raw data collected by the transducer array is transformed into valuable diagnostic information, playing a pivotal role in the deployment of UST for lung condition monitoring.

Figure 4. *UST device – panel view*

Creating the third version of the ultrasound tomography machine, which will be called Ultrasound Tomography 3.0 from now on, was a big step forward in the non-invasive study of how crystals form. This document overviews the substantial work undertaken to enhance the device's capabilities. The UST device design was based on eight four-channel measurement cards. These cards were interconnected through a high-speed FD CAN bus system capable of transferring data at up to 8 MBPS rates. The measurement cards were engineered to achieve a maximum sampling rate of 4 MBPS per channel. Each channel was equipped with a dedicated generator for square alternating waveforms, with amplitudes reaching up to 144 Vp-p (volts peak-to-peak) and an instantaneous current output of 3A. One of the pivotal advancements in the device was the ability to sample the analog signal across all channels synchronously. This synchronous capability helped to improve imaging resolution and

accuracy. Additionally, each channel was integrated with three eight-order band-pass filters, effectively removing harmonics via analog switches. These filters were tailored to the specific frequencies of the ultrasonic transducers, namely 40 kHz, 350 kHz, and 1 MHz, each with respective bandwidths designed to match the operational frequencies.

The measurement cards also featured a built-in system capable of converting the alternating acoustic analog signal into its envelope, with configurable settings to accommodate the three primary frequency ranges. Moreover, the cards included a two-stage amplification adjustment for each channel, facilitating a broad range of signal enhancement, from subtle amplification to significant increases in signal strength. The measurement cards contained a 32-bit STM32G474RE microcontroller with a Cortex-M4 core and a maximum clock speed of 170 MHz, as well as 512 kB of Flash memory, 96 kB of SRAM, and specialized units for floating-point and digital signal processing. The central control unit, which managed the operations of the measurement cards, was based on the existing design from the Ultrasound Tomography 2.0 device but was now powered by a different microcontroller to support CAN-FD communication. This new microcontroller, a 32-bit STM32H743ZI with a Cortex-M7 core, was capable of reaching clock speeds up to 480 MHz and came with 2MB of flash memory and 1 MB of RAM, further enhancing the system's processing capabilities with advanced instruction sets for digital signal processing.

Complementing these hardware improvements, the user interface and image reconstruction system were designed to operate on a Raspberry Pi board with a 7-inch touchscreen display, marking a user-friendly transition in interfacing with the device. Significant modifications were made to the measurement card, which now featured a compact board size and was powered by the targeted STM32G474 microcontroller. As part of these changes, differential inputs from ADC converters were switched out for non-inverting and inverting inputs from built-in operational amplifiers. There were also more control outputs for analog switches and state signaling through LED indicators. The redesigned card included a 5-bit switch for addressing up to 63 different units. It featured a custom 3D-printed shield for the four-channel impulse generator, complete with a copper tape layer to provide effective electromagnetic shielding.

The primary device module was designed with versatility in mind, considering the dimensions of the FT811CB display, which was used exclusively during the prototype development phase. The STM32F746ZG microcontroller was replaced with the STM32H743ZI variant, which supported CAN FD communication at 8 MBPS and had much more processing power, with clock speeds of up to 480 MHz. This was a significant change from the previous ultrasound tomography model. In the finalized device, the graphical user interface (GUI) functions would be managed by a Raspberry Pi 4 board with a 7-inch touchscreen display. This main board also provided options for external memory connections, such as microSD cards and USB Fast Speed ports. It included battery backup for the real-time clock, backup registers, and FRAM memory. Communication with the computer could be established using USB High Speed 2.0 standards. Provision for a debugger connector, serial port, and various communication buses, such as FDCAN, SPI, and RS485, were made using a category 6a RJ45 connector. Additional I/O ports were made available through commonly used terminal strips.

Figure 5 displays an assembled high-voltage inverter on a control module board, a critical ultrasound tomography (UST) system component. This control board is the epicenter of the UST device, tasked with managing the electrical signals that drive the transducers responsible for emitting ultrasound waves.

Figure 5. *Assembled high-voltage inverter on the control module board*

The high-voltage inverter's role is to convert low-voltage DC power into the high-voltage AC power required by the ultrasound transducers.

Precision is critical in this conversion process, as the quality of the ultrasound signal directly impacts the resolution and accuracy of the lung images produced by the UST system. This board is meticulously outfitted with an array of electronic components, including microcontrollers, communication modules, and various connectors that facilitate the integration of the board into the broader UST system. These components work together to ensure the inverter operates within the necessary parameters, providing stable and reliable high-voltage outputs. In the context of the UST device, this control module board embodies the convergence of electronic engineering and medical technology, playing a foundational role in enabling non-invasive, high-resolution imaging of lung tissue.

Conclusions

The development of the presented UST device represents a significant technological leap forward in ultrasound imaging, tailored explicitly to the non-invasive study of crystallization processes. This project's culmination has resulted in a robust, sophisticated system characterized by high-speed, precise measurement capabilities and advanced signal processing. The third version of the ultrasonic measurement card incorporates numerous improvements based on findings from its predecessor, demonstrating a relentless commitment to enhancing performance and reliability. The refinements in card construction, such as replacing noisy power components, adding a more extensive array of addressing options, and shielding enhancements, have substantially reduced signal interference and noise. These advancements contribute to the increased accuracy and clarity of the images produced. Additionally, the central control unit's upgrades, featuring a more powerful microcontroller and versatile communication options, have significantly bolstered the system's processing power and operational flexibility. This has allowed for more complex tasks to be performed efficiently, opening up new possibilities in the scope and scale of imaging applications. Integrating a user-friendly interface and sophisticated image reconstruction capabilities on a Raspberry Pi platform emphasizes the system's focus on improving user interaction and operational

intuitiveness. This approach is expected to streamline the user experience, making the technology more accessible to a broader range of operators, from researchers to medical professionals. Furthermore, the project's forward-thinking design, evidenced by including a high-voltage inverter module, positions the system for future enhancements. This module's innovative features, such as its isolated DC-DC converters with variable voltage outputs, enhance the device's safety and provide a scalable solution for power requirements. In conclusion, the UST device is a testament to the progress in medical imaging technology. Its comprehensive design and operational improvements have laid a solid foundation for the future of non-invasive ultrasound imaging, promising more significant advancements in medical diagnostics and a deeper understanding of crystallization processes. The success of this project marks a significant milestone and sets the stage for further innovations that will continue to push the boundaries of what is possible in ultrasound tomography.

References

Bal, G., Chung, F. J., Schotland, J. C. (2015). Ultrasound modulated bioluminescence tomography and controllability of the radiative transport equation. *SIAM Journal on Mathematical Analysis*, *48*(2), 1332–1347. https://doi.org/10.1137/15M1026262

Cueto, C., Bates, O., Strong, G., Cudeiro, J., Luporini, F., Agudo, O. C., Gorman, G., Guasch, L., Tang, M.-X. (2021). Stride: a flexible platform for high-performance ultrasound computed tomography. *Computer Methods and Programs in Biomedicine*, *221*. https://doi.org/10.1016/j.cmpb.2022.106855

Dai, H., Penwarden, M., Kirby, R. M., Joshi, S. (2023). *Neural Operator Learning for Ultrasound Tomography Inversion*. https://arxiv.org/abs/2304.03297v2

Javaherian, A., Lucka, F., Cox, B. T. (2020). Refraction-corrected ray-based inversion for three-dimensional ultrasound tomography of the breast. *Inverse Problems*, *36*(12), 125010. https://doi.org/10.1088/1361-6420/ABC0FC

Khairi, M. T. M., Ibrahim, S., Yunus, M. A. M., Faramarzi, M., Sean, G. P., Pusppanathan, J., Abid, A. (2019). Ultrasound computed tomography for material inspection: Principles, design and applications. *Measurement*, *146*, 490–523. https://doi.org/10.1016/J.MEASUREMENT.2019.06.053

Koulountzios, P., Rymarczyk, T., Soleimani, M. (2021). A Triple-Modality Ultrasound Computed Tomography Based on Full-Waveform Data for Industrial Processes. *IEEE Sensors Journal*, *21*(18), 20896–20909. https://doi.org/10.1109/JSEN.2021.3100391

Laitinen, T., Lyyra-Laitinen, T., Huopio, H., Vauhkonen, I., Halonen, T., Hartikainen, J., Niskanen, L., Laakso, M. (2008). Electrocardiographic alterations during hyperinsulinemic hypoglycemia in healthy subjects. *Annals of Noninvasive Electrocardiology*, *13*(2), 97–105. https://doi.org/10.1111/j.1542-474X.2008.00208.x

Mazurek, M., Rymarczyk, T., Kania, K., Kłosowski, G. (2020). Dedicated algorithm based on discrete cosine transform for the analysis of industrial processes using ultrasound tomography. *Adjunct Proceedings of the 2020 ACM International Joint Conference on Pervasive and Ubiquitous Computing and Proceedings of the 2020 ACM International Symposium on Wearable Computers*, 82–85. https://doi.org/10.1145/3410530.3414381

Nagafune, K., Watanabe, S., Shioya, H. (2014). An evolutionary multi-criterion optimization approach utilizing the characteristics of strength distribution for sparse CT image reconstruction. *2014 Joint 7th International Conference on Soft Computing and Intelligent Systems, SCIS 2014 and 15th International Symposium on Advanced Intelligent Systems, ISIS 2014*, 353–358. https://doi.org/10.1109/SCIS-ISIS.2014.7044771

Qiu, W., Bouakaz, A., Konofagou, E. E., Zheng, H. (2021). Ultrasound for the Brain: A Review of Physical and Engineering Principles, and Clinical Applications. *IEEE Transactions on Ultrasonics, Ferroelectrics, and Frequency Control*, *68*(1). https://doi.org/10.1109/TUFFC.2020.3019932

Romanowski, A., Łuczak, P., Grudzień, K. (2019). X-ray imaging analysis of silo flow parameters based on trace particles using targeted crowdsourcing. *Sensors (Switzerland)*, *19*(15). https://doi.org/10.3390/s19153317

Rymarczyk, T. (2019). *Tomographic imaging in environmental, industrial and medical applications* (1st ed.). Wydawnictwo Naukowe Innovatio Press.

Schork, N. (2018). Randomized clinical trials and personalized medicine. *Soc. Sci. Med. 1982*, *210*, 71–73.

Shanghai, J., Shuang, Y., Hong, G., Shenghui, S., Binbin, L., Xinyu, H., Xue, Z., Mingfu, Z. (2021). Study on Reconstruction Algorithm of X-ray Fluorescence Computed Tomography based on L1/2-norm and Expectation-Maximum. *2021 19th International Conference on Optical Communications and Networks (ICOCN)*, 1–3. https://doi.org/10.1109/ICOCN53177.2021.9563774

Soleimani, M., Rymarczyk, T. (2023). Ultrasound Tomography for Lung Imaging: An Experimental Phantom Study. *IEEE Sensors Journal*, *23*(8). https://doi.org/10.1109/JSEN.2023.3252340

Tan, C., Jia, H., Liang, G., Wang, X., Niu, W., Dong, F. (2023). Combinational Multimodality Tomography System for Industrial Multiphase Flow Imaging. *IEEE Trans. Instrum. Meas.*, *72*, 1–10. https://doi.org/10.1109/TIM.2023.3309361

Tutschek, B., Braun, T., Chantraine, F., Henrich, W. (2017). Computed tomography and ultrasound to determine fetal head station. *Ultrasound in Obstetrics Gynecology*, *49*(2), 279–280. https://doi.org/10.1002/UOG.17291

Wilson, J., Patwari, N. (2010). Radio tomographic imaging with wireless networks. *IEEE Transactions on Mobile Computing*, *9*(5), 621–632. https://doi.org/10.1109/TMC.2009.174

Yetisen, A. K., Martinez-Hurtado, J. L., Ünal, B., Khademhosseini, A., Butt, H. (2018). Wearables in Medicine. In *Advanced Materials* (Vol. 30, Issue 33). Wiley-VCH Verlag. https://doi.org/10.1002/adma.201706910

Yigitler, H., Jantti, R., Kaltiokallio, O., Patwari, N. (2017). Detector Based Radio Tomographic Imaging. *IEEE Transactions on Mobile Computing*, *17*(1). https://doi.org/10.1109/tmc.2017.2699634

Zhang, Q., Xiao, Y., Dai, W., Suo, J., Wang, C., Shi, J., Zheng, H. (2016). Deep learning based classification of breast tumors with shear-wave elastography. *Ultrasonics*, *72*, 150–157. https://doi.org/10.1016/J.ULTRAS.2016.08.004

Zhao, R., Yan, R., Chen, Z., Mao, K., Wang, P., Gao, R. X. (2019). Deep learning and its applications to machine health monitoring. *Mechanical Systems and Signal Processing*, *115*, 213–237. https://doi.org/10.1016/J.YMSSP.2018.05.050